IEEE Access
Multidisciplinary | Rapid Review | Open Access Journal

Received May 25, 2020, accepted June 15, 2020, date of publication June 25, 2020, date of current version July 13, 2020.

*Digital Object Identifier 10.1109/ACCESS.2020.3004928*

# Robust and Adaptive Path-Following Control of an Underactuated Ship

**ZENON ZWIERZEWICZ**
Department of Marine Automation, Maritime University of Szczecin, 70-500 Szczecin, Poland
e-mail: z.zwierzewicz@am.szczecin.pl

This work was supported in part by the Research Program 1/S/KAO/20.

**ABSTRACT** The design of a vessel path-following control system based on a full, realistic, nonlinear model is considered. The control objective is to force a surface, course-unstable vessel to track a predefined geometric path. We study an underactuated ship characterized only by a surge control force and yaw control moment, typical of many supply vessels. The assumption is made that the ship's model parameters are unknown, while significant external disturbances and unmodeled dynamics exist. Therefore, the design procedures make use of robust and adaptive control techniques. The controller synthesis uses adaptive output feedback linearization and $H_\infty$ optimal control techniques. In this way, the proposed control scheme assures position tracking despite various uncertainties. Because the considered design method leads to a nonminimum phase system, the problem of how to stabilize unstable zero dynamics arises. The presented simulations are based on a realistic ship model in terms of the structure and experimentally identified parameters. The simulations illustrate the effectiveness of the proposed algorithms.

**INDEX TERMS** Adaptive systems, control design, H infinity control, mathematical model, nonlinear control systems, vehicle routing.

## I. INTRODUCTION

Path following requires an automatic control device to be designed so that it will able to steer the vessel by proper rudder actions in order to maintain a preset reference path that a route guidance system can generate [1].

Numerous advanced and precise guidance systems have been designed [2], [3], but due to harsh and hardly predictable sea conditions, the problem remains at present.

In reality, one has to deal with various uncertainties, such as inaccuracies of the system model and random events such as wind, current, waves and other external factors. In addition, the ship examined in this study (according to the specific model parameters) is unstable in terms of course keeping.

The design of a ship steering system therefore requires techniques that account for nonlinear effects and uncertainties. We address a ship model's parametric uncertainty, as well as unstructured internal and external disturbances. These include the environmental impact, model approximation errors and path-segment changes.

Most of the numerous approaches to tackling the problem of ship path following, or trajectory-tracking, make use of oversimplified models or suggest complex algorithms, so they should be considered theoretical studies, not practically functional designs.

The LQG approach to the track control of ships, based on the simple Nomoto model and Kalman filter, is addressed in [4]. In [5], surface ship path control is considered via the geometric control theory, leading to a nonminimum phase system. A sliding mode controller is designed to ensure system robustness and performance. Hui and Jihong [6] presented a controller based on virtual target guidance in the Serret-Frenet frame. The study [7] proposed the path-following problem for systems characterized by unstable zero dynamics.

Recently, many publications have addressed these issues based on the Lyapunov theory. In particular, the backstepping method has been popular, e.g., in [8], [9]. However, the resultant solutions seem quite sophisticated – not only complicated in structure but also expensive in terms of computation.

This article presents robust and adaptive control concepts solving the previously formulated problem of ship path following. The main aim of the work is to design a controller that will keep the ship on the path based on a realistic ship model with three degrees of freedom [1]. Its linearized

The associate editor coordinating the review of this manuscript and approving it for publication was Nishant Unnikrishnan.

version serves as the basis for the design of the controller. The controller developed herein, a robust and adaptive version of the standard feedback linearizing controller [10], guarantees position tracking in the presence of various uncertainties.

To approximate the system unknown dynamics, an approximator-like structure of model basis functions is used. The structure stores the knowledge contained in the general model [11]. Then, we use adaptive control to adjust the assumed structure of the model by tuning the parameters. Eventually, the $H_\infty$ control term is introduced, compensating for unstructured inaccuracies of modeling and external disturbances.

The ship model under consideration, which is experimentally validated, was identified due to its structure and parameters [12], [13]. The new results presented here in relation to [13] are based on the fact that the proposed controller (as a robust-adaptive controller) does not require knowledge of model parameters. Moreover, since it has an internal built-in mechanism to eliminate steady-state error due to unmatched disturbances, it does not require additional integral action. Otherwise, to cope with this problem, the integral dynamics of the path error should be introduced, making the controller design more complicated, and the system performance cannot be guaranteed.

The use of I/O linearization when some uncertainties, such as disturbing forces and modeling errors, exist causes the cancellations through nonlinear feedback to be inaccurate and the control results to be unsatisfactory. In fact, we employ I/O linearization for the linear system, which cancels only linear parts of the nonlinearities occurring here. This raises the order of unmodeled dynamics or, following a different interpretation, imposes additional disturbances. The use of adaptive and robust techniques is a good approach to solving such a problem. The assumed simplifications facilitating the design process [14] seem to be rational.

The essential issue that impacts the I/O linearization procedure is that the dynamics of the system under consideration is split into external and internal parts. The possible instability of internal dynamics is a crucial problem [15] that needs to be examined thoroughly, particularly because the system turns out to have unstable internal dynamics. One solution is to apply the technique of redefining the output [5], [7], [10].

The paper consists of six sections followed by the conclusions and an appendix. Section II provides preliminaries regarding robust and adaptive control, while Section III defines the ship path-following control problem. The model of ship dynamics in a mathematical form is demonstrated in Section IV. The techniques of I/O linearization and controller design are presented in Section V. Section VI includes a simulation study and briefly analyzes the results.

## II. PRELIMINARIES ON ROBUST AND ADAPTIVE CONTROL

This section presents some basic concepts and the main theorem that are used in solving the above-defined ship control problem.

### A. GENERAL FORMULATIONS

Let us take a nonlinear n*th*-order SISO system

$$\begin{aligned} x^{(n)} &= f(x, \dot{x}, \cdots, x^{(n-1)}) + g(x, \dot{x}, \cdots, x^{(n-1)})u + d \\ y &= x, \end{aligned} \tag{1}$$

where $f$ and $g$ are unknown but bounded continuous functions, $u \in \mathbb{R}$ is the control input, and $y \in \mathbb{R}$ is the system output. $d$ denotes external unknown disturbances, also assumed to be bounded. Let $\boldsymbol{x} = [x, \ \dot{x}, \ \cdots, x^{(n-1)}]^T \in \mathbb{R}^n$ be the state vector of the system. The control aim is to force the system's output $y$ to follow a given bounded reference signal $y_d$.

For an accurate system model not affected by any disturbances $d$, i.e., for known functions $f$ and $g$, and for no disturbances $d$, the insertion of a simple output-feedback-linearizing controller

$$u = g^{-1}(\boldsymbol{x})[-f(\boldsymbol{x}) - \boldsymbol{k}^T \boldsymbol{e} + y_d^{(n)}] \tag{2}$$

into the system (1) cancels exactly the two nonlinearities ($f$ and $g$) and brings the closed-loop dynamics to the form

$$e^{(n)} + k_n e^{(n-1)} + \cdots + k_1 e = 0 \tag{3}$$

where $e := y - y_d$ is the output tracking error and $\boldsymbol{k} = [k_1, \ k_2, \cdots, k_n]^T \in \mathbb{R}^n$ is the vector of coefficients.

By properly choosing the coefficients $k_i$ we can make this system asymptotically stable. For (1) to be controllable, we assume also that $g(\boldsymbol{x}) \neq 0, \forall \boldsymbol{x} \in U_c \subset \mathbb{R}^n$, where $U_c$ is a controllability region.

Let us now consider a real situation with active disturbances $d$ and in which the functions $f$ and $g$ are replaced respectively by a linearly parameterized approximation structures $\hat{f}(\boldsymbol{x}, \boldsymbol{\theta}^f) = \boldsymbol{\theta}^{fT} \boldsymbol{w}^f$, $\hat{g}(\boldsymbol{x}, \boldsymbol{\theta}^g) = \boldsymbol{\theta}^{gT} \boldsymbol{w}^g$ where

$$\boldsymbol{w}^f = [f_1, \ f_2, \cdots, f_{n_1}]^T, \quad \boldsymbol{w}^g = [g_1, \ g_2, \cdots, g_{n_2}]^T \tag{4}$$

are model basis functions [11] and

$$\begin{aligned} \boldsymbol{\theta}^f &= \left[\theta_1^f, \ \theta_2^f, \cdots, \theta_{n_1}^f\right]^T, \\ \boldsymbol{\theta}^g &= \left[\theta_1^g, \ \theta_2^g, \cdots, \theta_{n_2}^g\right]^T \end{aligned} \tag{5}$$

are unknown vectors of the system parameters.

Because only the estimates $\hat{\boldsymbol{\theta}}^f, \hat{\boldsymbol{\theta}}^g$ are accessible, the approximate nonlinear functions of the system (1) can be written in this form:,

$$\hat{f}(\boldsymbol{x}, \hat{\boldsymbol{\theta}}^f) = \hat{\boldsymbol{\theta}}^{fT} \boldsymbol{w}^f, \quad \hat{g}(\boldsymbol{x}, \hat{\boldsymbol{\theta}}^g) = \hat{\boldsymbol{\theta}}^{gT} \boldsymbol{w}^g. \tag{6}$$

Consequently, the certainty equivalent controller [16], [17] obtains this form:

$$u = \hat{g}^{-1}(\boldsymbol{x}, \hat{\boldsymbol{\theta}}^g)[-\hat{f}(\boldsymbol{x}, \hat{\boldsymbol{\theta}}^f) - \boldsymbol{k}^T \boldsymbol{e} + y_d^{(n)} + u_a]. \tag{7}$$

The sub-control $u_a$ attenuates external disturbances $d$ and the error due to function approximation while adaptive control is used.

The insertion of Equation (7) into to Equation (1) and transformation yields the tracking error dynamic equation

$$\begin{aligned} e^{(n)} = -\boldsymbol{k}^T \boldsymbol{e} + [(f(\boldsymbol{x}) - \hat{f}(\boldsymbol{x}, \hat{\boldsymbol{\theta}}^f)) \\ + (g(\boldsymbol{x}) - \hat{g}(\boldsymbol{x}, \hat{\boldsymbol{\theta}}^g))u] + u_a + d \end{aligned} \tag{8}$$

or, correspondingly,

$$\dot{\boldsymbol{e}} = \boldsymbol{A}\boldsymbol{e} + \boldsymbol{B}u_a + \boldsymbol{B}[(f(\boldsymbol{x}) - \hat{f}(\boldsymbol{x}, \hat{\boldsymbol{\theta}}^f)) + (g(\boldsymbol{x}) - \hat{g}(\boldsymbol{x}, \hat{\boldsymbol{\theta}}^g))u] + \boldsymbol{B}d, \quad (9)$$

where

$$\boldsymbol{A} = \begin{bmatrix} 0 & 1 & \cdots & 0 \\ 0 & 0 & \vdots & 0 \\ \vdots & \vdots & \ddots & \vdots \\ -k_1 & -k_2 & \cdots & -k_n \end{bmatrix}; \quad \boldsymbol{B} = \begin{bmatrix} 0 \\ 0 \\ \vdots \\ 1 \end{bmatrix}, \quad \boldsymbol{e} = \left[e, \dot{e}, \cdots, e^{n-1}\right]^T = [e_1, e_2, \cdots, e_n]^T. \quad (10)$$

Let us define the optimal parameter estimates as

$$\begin{aligned} \boldsymbol{\theta}^{f*} &= \arg\min_{\boldsymbol{\theta}^f \in \Omega_f} [\sup_{\boldsymbol{x} \in \Omega_x} \left\| f(\boldsymbol{x}) - \hat{f}(\boldsymbol{x}, \boldsymbol{\theta}^f) \right\|] \\ \boldsymbol{\theta}^{g*} &= \arg\min_{\boldsymbol{\theta}^g \in \Omega_g} [\sup_{\boldsymbol{x} \in \Omega_x} \left\| g(\boldsymbol{x}) - \hat{g}(\boldsymbol{x}, \boldsymbol{\theta}^g) \right\|] \end{aligned} \quad (11)$$

where $\Omega_f$, $\Omega_g$ and $\Omega_x$ are the sets of suitable bounds on $\boldsymbol{\theta}^f$, $\boldsymbol{\theta}^g$ and $\boldsymbol{x}$ respectively. We assume that $\boldsymbol{\theta}^f$, $\boldsymbol{\theta}^g$ and $\boldsymbol{x}$ never reach the boundary of $\Omega_f$, $\Omega_g$ and $\Omega_x$.

The minimum (residual) approximation error is defined as

$$d_e = (f(\boldsymbol{x}) - \hat{f}(\boldsymbol{x}, \boldsymbol{\theta}^{f*})) + (g(\boldsymbol{x}) - \hat{g}(\boldsymbol{x}, \boldsymbol{\theta}^{g*}))u. \quad (12)$$

In addition, assuming that the adopted approximator structure and the approximation domain render the $d_e$ bounded, we can rewrite the tracking error dynamic equation (9):

$$\dot{\boldsymbol{e}} = \boldsymbol{A}\boldsymbol{e} + \boldsymbol{B}u_a + \boldsymbol{B}[(\hat{f}(\boldsymbol{x}, \boldsymbol{\theta}^{f*}) - \hat{f}(\boldsymbol{x}, \hat{\boldsymbol{\theta}}^f)) + (\hat{g}(\boldsymbol{x}, \boldsymbol{\theta}^{g*}) - \hat{g}(\boldsymbol{x}, \hat{\boldsymbol{\theta}}^g))u] + \boldsymbol{B}[d_e + d] \quad (13)$$

or

$$\dot{\boldsymbol{e}} = \boldsymbol{A}\boldsymbol{e} + \boldsymbol{B}u_a + \boldsymbol{B}[\tilde{\boldsymbol{\theta}}^{fT}\boldsymbol{w}^f + \tilde{\boldsymbol{\theta}}^{gT}\boldsymbol{w}^g u] + \boldsymbol{B}\tilde{\boldsymbol{d}} \quad (14)$$

where $\tilde{d} = d_e + d$ are total disturbances and $\tilde{\boldsymbol{\theta}}^f = \boldsymbol{\theta}^{f*} - \hat{\boldsymbol{\theta}}^f$, $\tilde{\boldsymbol{\theta}}^g = \boldsymbol{\theta}^{g*} - \hat{\boldsymbol{\theta}}^g$.

Let us define the performance output

$$\boldsymbol{z} = \boldsymbol{C}\boldsymbol{e} + \boldsymbol{D}u_a. \quad (15)$$

In the above equation, to avoid cross terms on the left-hand side of the integrand of (17), we set $\boldsymbol{D}^T\boldsymbol{C} = \boldsymbol{0}$.

For further considerations, let us define that

$$\boldsymbol{Q} = \boldsymbol{C}^T\boldsymbol{C}, \quad r = \boldsymbol{R} = \boldsymbol{D}^T\boldsymbol{D}. \quad (16)$$

The design goal is to find a sub-controller $u_a$ and parameter adaptation laws for $\hat{\boldsymbol{\theta}}^f$, $\hat{\boldsymbol{\theta}}^g$ (compare (7)) that will allow to achieve $H_\infty$ tracking performance under the worst-case disturbances $\tilde{d}$:

$$\int_0^T (\boldsymbol{e}^T\boldsymbol{Q}\boldsymbol{e} + ru_a^2)dt \le \boldsymbol{e}^T(0)\boldsymbol{P}\boldsymbol{e}(0) + \frac{1}{\gamma_1}\tilde{\boldsymbol{\theta}}^{fT}(0)\,\tilde{\boldsymbol{\theta}}^f(0) + \frac{1}{\gamma_2}\tilde{\boldsymbol{\theta}}^{gT}(0)\tilde{\boldsymbol{\theta}}^g(0) + \rho^2\int_0^T \tilde{d}^2 dt \quad (17)$$

$\forall T \in [0, \infty)$ and $\boldsymbol{P} = \boldsymbol{P}^T > 0, \tilde{d} \in L_2[0, T]$

The adaptation gains are $\gamma_i > 0$, while $\rho$ is a predefined attenuation level (for more details, see [16], [17]).

If the system starts under initial conditions $\boldsymbol{e}(0) = 0$ $\tilde{\boldsymbol{\theta}}^f(0) = 0$, $\tilde{\boldsymbol{\theta}}^g(0) = 0$, the inequality (17) means that the $L_2$ gain [18] from $\tilde{d}$ to the tracking performance output $z(t)$ ($\|z(t)\|_2^2 = \int_0^T (\boldsymbol{e}^T\boldsymbol{Q}\boldsymbol{e} + ru_a^2)\,dt$) is less or equal to $\rho$, i.e.,

$$\|z(t)\|_2 \le \rho \left\|\tilde{d}(t)\right\|_2. \quad (18)$$

To obtain the optimal tracking performance $H_\infty$, we aim to reach the minimal attenuation level $\rho^*$.

### B. THE MAIN THEOREM

The solution of the above problem can be explained by the following theorem.

*Theorem:* If we choose in the nonlinear system (1) the robust-adaptive control law

$$u = \frac{1}{\hat{\boldsymbol{\theta}}^{gT}\boldsymbol{w}^g}\left[-\hat{\boldsymbol{\theta}}^{fT}\boldsymbol{w}^f - \boldsymbol{k}^T\boldsymbol{e} + y_d^{(n)} + u_a\right] \quad (19)$$

with the robustifying term

$$u_a = -\frac{1}{r}\boldsymbol{B}^T\boldsymbol{P}\boldsymbol{e} \quad (20)$$

and adaptive parameter tunings of the form

$$\begin{aligned} \dot{\hat{\boldsymbol{\theta}}}^f &= \gamma_1\boldsymbol{w}^f\boldsymbol{B}^T\boldsymbol{P}\boldsymbol{e} \\ \dot{\hat{\boldsymbol{\theta}}}^g &= \gamma_2\boldsymbol{w}^g\boldsymbol{B}^T\boldsymbol{P}\boldsymbol{e}u \end{aligned} \quad (21)$$

where $r$ is a positive scalar value and $\boldsymbol{P} = \boldsymbol{P}^T > 0$ is the solution of the following Riccati-like equation

$$\boldsymbol{P}\boldsymbol{A} + \boldsymbol{A}^T\boldsymbol{P} + \boldsymbol{Q} - \frac{1}{r}\boldsymbol{P}\boldsymbol{B}\boldsymbol{B}^T\boldsymbol{P} + \frac{1}{\rho^2}\boldsymbol{P}\boldsymbol{B}\boldsymbol{B}^T\boldsymbol{P} = \boldsymbol{0}, \quad (22)$$

then the $H_\infty$ tracking performance (17) is achieved for the preset attenuation level $\rho$. □

*Remark 1:* Assuming that there exists a positive constant $M$ such that $\int_0^\infty \tilde{d}^2 dt \le M$, we obtain the bounded integral $\int_0^\infty (\boldsymbol{e}^T\boldsymbol{Q}\boldsymbol{e} + ru_a^2)dt$ from (17). According to Barbalat's Lemma [10], we can then infer that $\lim_{t\to\infty} \boldsymbol{e}(t) = 0$. The proof of this theorem as well as its variant that addresses the parameter drift problem, via the $\sigma$-modification method, is given in the Appendix. In this version the formulas (21) should be replaced by (8A) and the condition (18A), guaranteeing system stabilizability i.e. that $\hat{g}(\boldsymbol{x}, \hat{\boldsymbol{\theta}}^g)$ of (7) is bounded away from zero, should be also considered.

## III. SHIP PATH-FOLLOWING CONTROL PROBLEM

This part defines the main problem of ship control along a preset reference track. The planned track is normally defined by waypoints. The ship proceeds at a constant speed $U$, while the sway position $y$ is controlled (Figure 1). The purpose of following a waypoint route is to control the angle of heading and the displacement of the sway, changing only the rudder deflection. In general, in the case of a typical underactuated vessel (more degrees of freedom have to be controlled

than the number of independent control devices), the only feasible thing to do is to impact the sway position along the reference path and accept the course error. Therefore, as various uncertainties exist, we can only ensure position tracking.

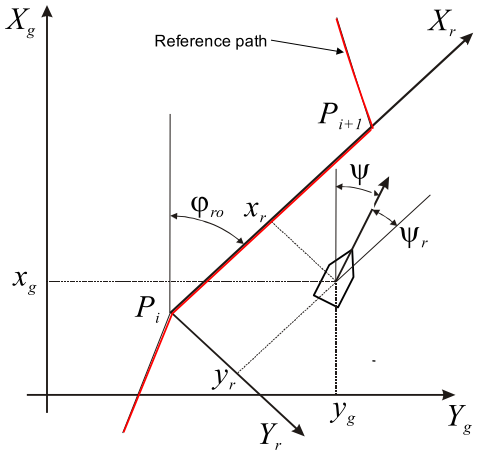


**FIGURE 1.** Earth-fixed and relative coordinate systems.

### A. DEFINITION OF PATH-FOLLOWING ERRORS

Let us make an assumption that the path to be tracked consists of sections of a broken line defined by a sequence of vertices (turn points) $P_1(x_1, y_1), P_2(x_2, y_2), \ldots, P_i(x_i, y_i), \ldots, P_n(x_n, y_n)$. We will also specify the coordinate systems as follows (Fig. 1):

- earth-fixed coordinate system $(X_g, Y_g)$ (where the coordinates are determined by the GPS),
- a relative coordinate system $(X_r, Y_r)$ with the origin placed at point $P_i(x_i, y_i)$ and the axis $OX_r$ runs along $P_iP_{i+1} (i = 1, 2, \ldots, n)$.

Let the transformations

$$\begin{bmatrix} x_r \\ y_r \\ \psi_r \end{bmatrix} = \begin{bmatrix} \cos\phi_{ro} & \sin\phi_{ro} & 0 \\ -\sin\phi_{ro} & \cos\phi_{ro} & 0 \\ 0 & 0 & 1 \end{bmatrix} \begin{bmatrix} x_g - x_i \\ y_g - y_i \\ \psi - \phi_{ro} \end{bmatrix} \tag{23}$$

$$\tan\phi_{ro} = \frac{y_{i+1} - y_i}{x_{i+1} - x_i}. \tag{24}$$

define the relative ship position $(x_r, y_r)$ and its relative heading $\psi_r$ ($\phi_{ro}$ is an angle of the system $(X_g, Y_g)$ rotation).

Now, we can define tracking errors for a given path segment:

- $y_r$ cross track error
- $\psi_r$ heading error

These variables will be further treated as path-following errors that correspond to a given segment.

For a curvilinear reference path, the local (relative) coordinate system should be tangent to the path at the point that is closest to the present ship position. This system has to then be shifted and rotated from time step to time step in such a way that it remains tangent to the reference path and that the $x$-coordinate represents the arc length along the path.

## IV. MATHEMATICAL MODEL OF SHIP DYNAMICS

### A. GENERAL MODEL STRUCTURE

We present below a general nonlinear model of the ship, further employed as a model simulating its real dynamics. This model is also used to derive a simplified, linear model that will facilitate controller design.

The state variables that represent the ship's movement are defined by two vectors $\boldsymbol{\eta} = [x, y, \psi]^T$ and $\boldsymbol{\nu} = [u, v, r]^T$, where $(x, y)$ are the coordinates of ship's position; $\psi$ is the vessel heading; $(u, v)$ are linear, body-fixed speeds (surge, sway); and $r$ is the rate of turn.

The general mathematical representation of the ship dynamics is expressed by this equation [1], [19]:

$$\boldsymbol{M}\dot{\boldsymbol{\nu}} + \boldsymbol{C}(\boldsymbol{\nu})\boldsymbol{\nu} + \boldsymbol{D}(\boldsymbol{\nu})\boldsymbol{\nu} = \boldsymbol{\tau} \tag{25}$$

where $\boldsymbol{M}$ is the positive definite inertia mass matrix, including the added mass,

$$\boldsymbol{M} = \begin{bmatrix} m - X_{\dot{u}} & 0 & 0 \\ 0 & m - Y_{\dot{v}} & mx_G - Y_{\dot{r}} \\ 0 & mx_G - N_{\dot{v}} & I_z - N_{\dot{r}} \end{bmatrix}, \tag{26}$$

and $\boldsymbol{C}(\boldsymbol{\nu})$ stands for the Coriolis centripetal matrix,

$$\boldsymbol{C} = \begin{bmatrix} 0 & 0 & -c_{31} \\ 0 & 0 & (m - X_{\dot{u}})u \\ c_{31} & (m - X_{\dot{u}})u & 0 \end{bmatrix}, \tag{27}$$

where $c_{31} = (mx_G - Y_{\dot{r}})r + (m - Y_{\dot{v}})v$.

$\boldsymbol{D}(\boldsymbol{\nu})$ is the damping matrix, $\boldsymbol{\tau} = [\tau_X, \tau_Y, \tau_N]^T$ is the vector of forces and moment that affect the ship movement,

$$\boldsymbol{D}(\boldsymbol{\nu}) = \begin{bmatrix} -d_{11}(\boldsymbol{\nu}) & 0 & 0 \\ 0 & -d_{22}(\boldsymbol{\nu}) & -d_{23}(\boldsymbol{\nu}) \\ 0 & -d_{32}(\boldsymbol{\nu}) & -d_{33}(\boldsymbol{\nu}) \end{bmatrix}, \tag{28}$$

where

$$\begin{aligned} d_{11}(\boldsymbol{\nu}) &= X_{|u|u}\,|u| \\ d_{22}(\boldsymbol{\nu}) &= Y_{|u|v}\,|u| + Y_{|v|v}\,|v| + Y_{|r|v}\,|r| \\ d_{23}(\boldsymbol{\nu}) &= Y_{|u|r}\,|u| + Y_{|v|r}\,|v| + Y_{|r|r}\,|r| \\ d_{32}(\boldsymbol{\nu}) &= N_{|u|v}\,|u| + N_{|v|v}\,|v| + N_{|r|v}\,|r| \\ d_{33}(\boldsymbol{\nu}) &= N_{|u|r}\,|u| + N_{|v|r}\,|v| + N_{|r|r}\,|r|\,. \end{aligned} \tag{29}$$

Under the assumption that the surge $u = u_0 \approx$ constant, sway and yaw (i.e., $v$ and $r$) are sufficiently small, we can linearize the nonlinear matrix $\boldsymbol{D}(\boldsymbol{\nu})$ to obtain its linear counterpart $\boldsymbol{D}_L$ [19], [12]:

$$\boldsymbol{D} \approx \boldsymbol{D}_L = \begin{bmatrix} -X_u & 0 & 0 \\ 0 & -Y_v & -Y_r \\ 0 & -N_v & N_r \end{bmatrix} \tag{30}$$

For specific propeller revolutions and a fixed deflection angle of the rudder, the generated thrust force is roughly proportional to the square of the propeller rotational speed $n$, so the nominal, linearized thrust $\tau_X = X_n n$. The forces acting on the ship hull normally depend on the rudder deflection angle $\delta$, which is defined by the equations $\tau_Y = -Y_\delta \delta$ and $\tau_N = -N_\delta \delta$.

The components of the matrices (26), (27) and (30), known as hydrodynamic derivatives, are given in the appendix (Table 2). Determined through strict identification procedures, these figures refer to the training ship 'Blue Lady' (more details can be found in [12], [13]).

### B. DAVIDSON AND SCHIFF'S SIMPLIFIED LINEARIZED MODEL

Models (25)-(29) are significantly simplified when we take the linearized $\boldsymbol{D}_L$ version instead of the $\boldsymbol{D}$ matrix.

The longitudinal ship dynamics of the resultant model has the form

$$(m - X_{\dot{u}})\dot{u} = (m - Y_{\dot{v}})vr + (mx_G - Y_{\dot{r}})r^2 + X_u u + X_{|u|u}\,|u| \cdot u + \overbrace{X_n n}^{\tau_X}$$

while its transverse rotational dynamics is actually the Davidson and Schiff model [1]

$$\boldsymbol{M}_1\dot{\boldsymbol{v}}_1 + \boldsymbol{N}(u_0)\boldsymbol{v}_1 = \boldsymbol{G}\delta \tag{31}$$

where $\boldsymbol{v}_1 = \begin{bmatrix} v & r \end{bmatrix}^T$ and

$$\boldsymbol{M}_1 = \begin{bmatrix} m - Y_{\dot{v}} & mx_G - Y_{\dot{r}} \\ mx_G - N_{\dot{v}} & I_z - N_{\dot{r}} \end{bmatrix};$$

$$\boldsymbol{N}(u_0) = \begin{bmatrix} -Y_v & -Y_r + (m - X_{\dot{u}})u_0 \\ -N_v + (X_{\dot{u}} - Y_{\dot{v}})u_0 & N_r + (mx_G - Y_{\dot{r}})u_0 \end{bmatrix};$$

$$\boldsymbol{G} = \begin{bmatrix} Y_\delta \\ N_\delta \end{bmatrix}$$

or

$$\dot{\boldsymbol{v}}_1 = \boldsymbol{A}_1\boldsymbol{v}_1 + \boldsymbol{B}_1\delta, \tag{32}$$

where

$$\boldsymbol{A}_1 = \boldsymbol{M}_1^{-1}\boldsymbol{N}(u_0) = \begin{bmatrix} a_{11} & a_{12} \\ a_{21} & a_{22} \end{bmatrix}; \quad \boldsymbol{B}_1 = \boldsymbol{M}_1^{-1}\boldsymbol{G} = \begin{bmatrix} b_1 \\ b_2 \end{bmatrix}.$$

The model (31) outlined above makes up a basis for the final model (35) suitable for the control system design.

### C. THE MODEL FOR CONTROLLER DESIGN

The kinematic equations of vessel movement may be as below [1], [12]:

$$\begin{aligned} \dot{x} &= u\cos\psi - v\sin\psi \\ \dot{y} &= u\sin\psi + v\cos\psi \\ \dot{\psi} &= r. \end{aligned} \tag{33}$$

As linear approximation of (33), we take the equations

$$\dot{y}_r = U\psi_r + v + d_y; \quad \dot{\psi}_r = r \tag{34}$$

written in relation to the transformed (23) coordinates and assuming that $u \approx U$. The first kinematic equation in the model (33) is neglected because $x_r$ represents motion along the path, which is not relevant in our considerations.

The combination of equations (32) and (34) results in the linear model presented below, used for the controller design:

$$\begin{bmatrix} \dot{v} \\ \dot{r} \\ \dot{\psi}_r \\ \dot{y}_r \end{bmatrix} = \begin{bmatrix} a_{11} & a_{12} & 0 & 0 \\ a_{21} & a_{22} & 0 & 0 \\ 0 & 1 & 0 & 0 \\ 1 & 0 & U & 0 \end{bmatrix} \begin{bmatrix} v \\ r \\ \psi_r \\ y_r \end{bmatrix} + \begin{bmatrix} b_1 \\ b_2 \\ 0 \\ 0 \end{bmatrix} \delta + \begin{bmatrix} 0 & 0 \\ 1 & 0 \\ 0 & 0 \\ 0 & 1 \end{bmatrix} \begin{bmatrix} d_r \\ d_y \end{bmatrix} \tag{35}$$

with output

$$y = y_r \tag{36}$$

where

$y_r$ – relative abscissa of the ship position (cross-track error)

$\psi_r$ – relative heading (course-error)

$d_y$ – uncertain parameter because of modeling errors and sea currents

$d_r$- environmental disturbances (constant or slow-varying, wave/wind-induced torque).

## V. I/O LINEARIZATION AND CONTROLLER DESIGN

Because the system (35), (36), representing the controlled process, is nonminimum phase [10], after I/O linearization, part of the dynamics will be unstable. To solve this problem, we have to change the system structure or reformulate the task, e.g., through a new definition of the output [10], [14], [15].

### A. OUTPUT REDEFINITION

One of the methods allowing a change of the nonminimum phase system (35) into a minimum-phase system (a system characterized by asymptotically stable internal dynamics) is to redefine the new output [5] herein in this form:

$$y = y_r + k\psi_r, \tag{37}$$

where the constant $k$ ought to be chosen in such a way that the zeros of the transfer function (35), (37) are positioned in the left-half of the s-plane, thus providing for the stability of the system zero dynamics.

The reason for choosing the output (37) is that the helmsman maintaining the vessel on a planned path takes account of the cross-track error and the course.

### B. ZERO DYNAMIC

To analyze the system zero dynamics, it is enough to examine the original system (35), assuming that the output (37) is identically equal to zero $y(t) \equiv 0$. This leads to the system's restricted motion [20] confined to the set

$$\begin{aligned} Z^* &= \{x : h(x) = L_f h(x) = 0\} \\ &= \{x : y_r + k\psi_r = 0 \ \wedge \ U\psi_r + v + kr = 0\} \end{aligned} \tag{38}$$

The motion of the original system (35) on $Z^*$, with the input $\delta = \alpha(x) = -f(x)/g(x)$ (compare (41)), represents the zero dynamic.

To be more specific, by using (38) and the last two equations of (35), we can get, after simple calculations, the equation

$$y_r + k\psi_r = \tilde{C}, \tag{39}$$

which, after setting constant $\tilde{C}$ to zero, is identical to the left equation given in (38). This procedure proves that the last two equations of (35) are satisfied on the set $Z^*$.

The first two equations of (35) with $\delta = \alpha(x)$ constitute a linear system parametrized by $k$. This system represents the searched-for zero dynamic, which can be made asymptotically stable via appropriate selection of $k$.

The same reasoning can be followed in the case of system (35) with the output (36). However, the result obtained this time proves that the zero dynamics may be unstable.

### C. CONTROLLER DESIGN

To make the control synthesis based on the I/O linearization method and to avoid the formalism of Lie derivatives, we differentiate the new output (37) against time twice, obtaining the equations

$$\begin{aligned} \dot{y}_1 &= y_2 \\ \dot{y}_2 &= f(\boldsymbol{x}) + g(\boldsymbol{x})\delta, \end{aligned} \tag{40}$$

where $y = y_1 = y_r + k\psi_r$, $\dot{y} = y_2$

$$\begin{aligned} f(\boldsymbol{x}) &= (a_{11} + ka_{21})v + (U + a_{12} + ka_{22})r + \tilde{d} \\ g(\boldsymbol{x}) &= (b_1 + kb_2)\delta. \end{aligned} \tag{41}$$

In this context, $\tilde{d}$ is a total disturbance (i.e., disturbance and uncertainty combined), while the state vector $\boldsymbol{x} = [v,\ r,\ \psi_r,\ y_r]^T$ is regarded as measurable.

The partial transformation of the coordinates from $\boldsymbol{x}$ to $\boldsymbol{y}$ is defined by the equations

$$y_1 = y = y_r + k\psi_r, \quad y_2 = \dot{y}_r + k\dot{\psi}_r = U\psi_r + v + kr + d_y \tag{42}$$

After this transformation, we obtain a new system (40) of the second order, representing the external dynamics. As the original system (35) is of the 4$^{\text{th}}$ order, the missing part of the dynamics should be completed with the internal dynamics (of the 2$^{\text{nd}}$ order as well) analyzed above.

*Remark 2:* The question arises whether the ship (or its original nonlinear model) will also be a nonminimum-phase system – similarly to its linear counterpart. The affirmative answer, at least locally, results from a theoretical analysis [5] and actual physical restrictions (input-output stability imposes a stabilizing effect also on the inner state variables [12]).

The nonlinearities $f$, $g$ of (40) may be parametrized [11] as follows:

$$\begin{aligned} \hat{f}(\boldsymbol{x}, \hat{\boldsymbol{\theta}}) &= \sum_{i=1}^{3} \hat{\theta}_i^f f_i = \hat{\theta}_1^f v + \hat{\theta}_2^f r + \hat{\theta}_3^f \\ \hat{g}(\boldsymbol{x}, \hat{\boldsymbol{\theta}}) &= \sum_{i=1}^{1} \hat{\theta}_i^g g_i = \hat{\theta}_1^g. \end{aligned} \tag{43}$$

From these equations, we obtain a set of model basis functions $f_i$, $g_i$ and the corresponding parameters:

$$\begin{aligned} \boldsymbol{w}^f &= [v, r, 1], \quad & \hat{\boldsymbol{\theta}}^f &= [\hat{\theta}_1^f,\ \hat{\theta}_2^f,\ \hat{\theta}_3^f] \\ \boldsymbol{w}^g &= 1, & \hat{\boldsymbol{\theta}}^g &= \hat{\theta}_1^g, \end{aligned} \tag{44}$$

The controller (19) can now be written in the form:

$$\delta = (-\hat{\theta}_1^f v - \hat{\theta}_2^f r - \hat{\theta}_3^f - k_1 y_1 - k_2 y_2 + \delta_a)/\hat{\theta}_1^g. \tag{45}$$

A simple analysis indicates that this controller uses all information contained in the state vector $\boldsymbol{x}$, although some of it is used implicitly - through $y$ and $\dot{y}$ (42). The controller also executes integral action through parameter $\hat{\theta}_3^f$ (conf. *Remark 4*).

To obtain the final solution, we have to solve the Riccati-like equation (RE) (22). To this end, we insert the control (45) into (40) to yield the following formula

$$\begin{aligned} \begin{bmatrix} \dot{y}_1 \\ \dot{y}_2 \end{bmatrix} &= \underbrace{\begin{bmatrix} 0 & 1 \\ -k_1 & -k_2 \end{bmatrix}}_{\boldsymbol{A}} \underbrace{\begin{bmatrix} y_1 \\ y_2 \end{bmatrix}}_{\boldsymbol{y}} + \underbrace{\begin{bmatrix} 0 \\ 1 \end{bmatrix}}_{\boldsymbol{B}} \delta_a \\ &\quad + \begin{bmatrix} 0 \\ 1 \end{bmatrix} (\tilde{\boldsymbol{\theta}}^{fT} \boldsymbol{w}^f + \tilde{\boldsymbol{\theta}}^{gT} \boldsymbol{w}^g \delta) + \begin{bmatrix} 0 \\ 1 \end{bmatrix} \tilde{d} \end{aligned} \tag{46}$$

that defines matrices $\boldsymbol{A}$ and $\boldsymbol{B}$ required here.

The matrix $\boldsymbol{Q}$ and scalar $r$ can be received by writing the output (15) in the component form

$$\boldsymbol{z} = \begin{bmatrix} z_1 \\ z_2 \end{bmatrix} = \underbrace{\begin{bmatrix} \lambda & 0 \\ 0 & 0 \end{bmatrix}}_{C} \begin{bmatrix} y_1 \\ y_2 \end{bmatrix} + \underbrace{\begin{bmatrix} 0 \\ \sqrt{r} \end{bmatrix}}_{D} \delta_a = \begin{bmatrix} \lambda y_1 \\ \sqrt{r}\delta_a \end{bmatrix} \tag{47}$$

from which we can get matrices $\boldsymbol{C}$ and $\boldsymbol{D}$; consequently, $\boldsymbol{Q} = \boldsymbol{C}^T\boldsymbol{C}$, $r = \boldsymbol{R} = \boldsymbol{D}^T\boldsymbol{D}$.

Finally, using the Matlab function *care* [21], we can find the proper numerical solutions $\boldsymbol{P}$ of equation (22) for different values of the chosen attenuation level $\rho > 0$.

Since we wish $\rho$ to be minimal (on the condition that there is a solution to the RE), we have to use this procedure iteratively.

Knowing the matrix $\boldsymbol{P}$, we can obtain, according to (20), (21), both the robustifying term $\delta_a$ and the parameter tuning rules [14]:

$$\delta_a = -\frac{1}{r}\boldsymbol{B}^T\boldsymbol{P}\boldsymbol{y} = -\frac{\varepsilon}{r} \tag{48}$$

$$\begin{aligned} \dot{\hat{\theta}}_1^f &= \gamma_1 v \boldsymbol{B}^T\boldsymbol{P}\boldsymbol{e} = \gamma_1 v\varepsilon \\ \dot{\hat{\theta}}_2^f &= \gamma_2 r \boldsymbol{B}^T\boldsymbol{P}\boldsymbol{e} = \gamma_2 r\varepsilon \\ \dot{\hat{\theta}}_3^f &= \gamma_3 \boldsymbol{B}^T\boldsymbol{P}\boldsymbol{e} = \gamma_3\varepsilon \\ \dot{\hat{\theta}}_1^g &= \gamma_4 \boldsymbol{B}^T\boldsymbol{P}\boldsymbol{e} = \gamma_4\varepsilon\delta \end{aligned} \tag{49}$$

where $\boldsymbol{B}^T\boldsymbol{P}\boldsymbol{y} = p_{21}y_1 + p_{22}y_2 = \varepsilon$ and $\boldsymbol{P} = \boldsymbol{P}^T > 0$.

*Remark 3:* Note that, in the case of nonadaptive control

$$\delta = \frac{-(a_{11}+ka_{21})v - (U+a_{12}+ka_{22})r - k_1y_1 - k_2y_2}{b_1 + kb_2}, \tag{50}$$

(compare (41) and (45)), we can, by virtue of proper selection of parameter $k$, modify the closed loop system parameters to

obtain stable zero dynamics. In a similar manner, the steady-state parameters $\theta$ of controller (45) can be modified in the case of an adaptive system. It follows from the fact that the error $\varepsilon$ in (49) is a function of $k$.

It seems also that the existence of the feedback law for the considered geometric path following problem may be sanctioned by theorem 1 in [15].

*Remark 4:* Note that the tuning of parameter $\hat{\theta}_3^f$ (by the built-in integrating action) compensates for the constant component of the disturbances $\tilde{d}$, while the non-Gaussian part of disturbances, with bounded energy (decaying disturbances), is reduced by the robustifying term $\delta_a$. Since the integration employed here is put on the linear combination of the state vector components, this type of integral action (cf. equation (49)) can be called a generalized integral action. In this way, we can bring the old output (cross-track error) down to zero, regardless of active unmatched disturbances (e.g., sea current, waves, drift forces), provided that we use the error $\varepsilon = p_{21}y_r + p_{22}\dot{y}_r$ based on the old (35), (36) system transformed state components. This practice can be viewed as independent of the rest of the design procedure.

The baseline controller $\boldsymbol{k}^T\boldsymbol{y} = k_1y_1 + k_2y_2$ should be designed to guarantee the stability of system (46), in which the parametrical and external uncertainties are ignored. The controller gains $k_1$ and $k_2$ can be reached by, for instance, the lqr technique.

Observe that all the state components of the original system (35) are involved here (compare (42)). Notice also that $\dot{y}_r$ can be obtained via rotation of the ship-fixed coordinate system $(u,v)$, located at the ship's center of gravity. Consequently, all measurements needed to implement the controller are the position via GPS and course via gyrocompass, while the velocities can be calculated from them.

## VI. SIMULATION RESULTS

The simulations presented below, aimed at verifying the performance of the designed control system, are based on the general ship dynamical, nonlinear model (25). The model parameters were determined based on the identification process of the 'Blue Lady' training ship [13].

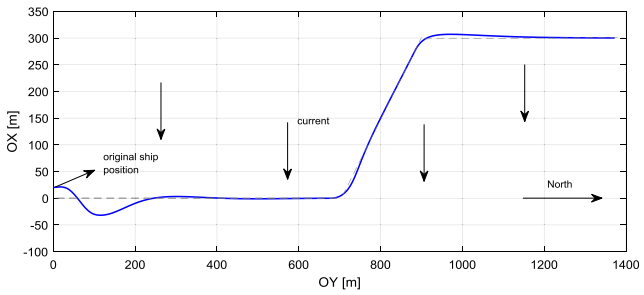


**FIGURE 2.** Ship trajectory in the xy plane.

Figure 2 shows the path as a broken line defined by the so-called waypoints (0,0), (0,700), (300,900) and (300,1400).

The vessel's initial position, heading and rate of turn (angular velocity) are (20.0), 30° and 0 rad/min, respectively. The assumed distance scale is 1 m, and the ship has a nominal speed of 0.7 m/s at constant propulsion.

As additional disturbances, transverse current ($d_y = -0.3$ m/s) and a torque $d_r$ induced by the wind (corresponding to a rudder deflection of 10°; Fig. 4) were considered.

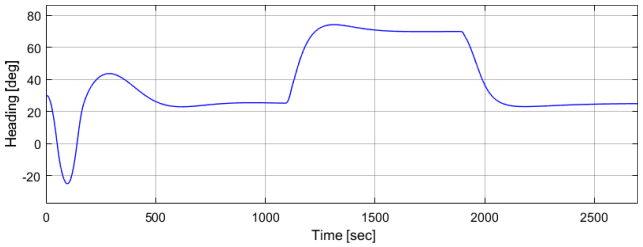


**FIGURE 3.** Ship headings versus time.

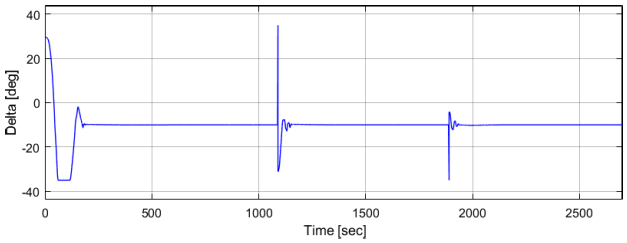


**FIGURE 4.** Rudder deflection versus time.

Fig. 3 depicts a plot of the ship's heading as a function of time. The heading of a ship moving along horizontal path sections (north) is approximately 25°, indicating a course error. This occurs because the examined vessel has only two actuators (rudder and propeller) responsible for steering, so it is underactuated, and only its surge and heading can be controlled.

The above behavior of the ship is necessary to compensate for the effect of currents. It should be borne in mind that the main function of the controller is to reduce the output, the cross-track error, to zero. Simultaneously bringing $\psi_r$ to zero in the presence of transverse current is sometimes impossible for a ship with the actuators assumed in this study. As a result, the process of following a specific path can only be affected when a course error occurs (we can get only the position tracking [3]).

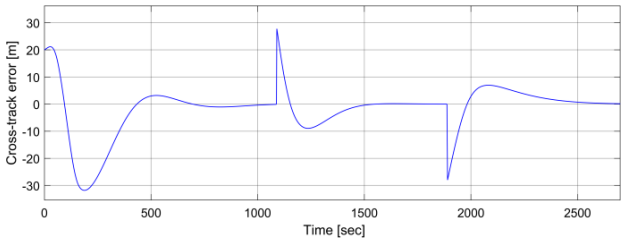


**FIGURE 5.** Cross-track errors versus time.

Figure 5 illustrates the cross-track error as a function of time. We can observe that our controller is capable of effectively compensating for the steady-state error created by

**TABLE 1. Main details of the blue lady ship.**

| | |
|---|---|
| Length overall [m] | 13.78 |
| Length between perpendiculars [m] | 13.50 |
| Breadth [m] | 2.38 |
| Mean draught (full load) [m] | 0.86 |
| Displacement (full load) [$m^3$] | 22.83 |
| Nominal $x$ coordinate of CG (xG) [m] | 0.00 |
| Maximum speed [knots] | 3.10 |

**TABLE 2. Parameters of the mathematical model of the Blue Lady.**

| | | |
|---|---|---|
| $m = 22\,934$ | $I_z = 436\,830$ | $X_{\dot{u}} = -731$ |
| $Y_{\dot{v}} = -18\,962$ | $Y_{\dot{r}} = -183\,519$ | $N_{\dot{v}} = 0.0$ |
| $N_{\dot{r}} = 0.0$ | $X_{\|u\|u} = 194$ | $Y_{\|u\|v} = 2\,351$ |
| $Y_{\|v\|v} = 6\,860$ | $Y_{\|r\|v} = 29\,635$ | $Y_{\|u\|r} = -7\,842$ |
| $Y_{\|v\|r} = -18\,522$ | $Y_{\|r\|r} = -12\,502$ | $N_{\|u\|v} = 0.0$ |
| $N_{\|v\|v} = 0.0$ | $N_{\|r\|v} = -40\,007$ | $N_{\|u\|r} = 55\,614$ |
| $N_{\|u\|v} = 12\,502$ | $N_{\|r\|r} = 843\,900$ | |
| $Y_\delta = -115.50$ | $N_\delta = 471.70$ | $X_n = 1.96$ |

combined disturbance moments due to unmodeled dynamics, external winds and changes in parameters.

As a criterion for selecting the moment of changing the coordinate system relative to a given path segment, it is assumed that the distance of the vessel to the turning point $P_i(x_i, y_i)$ is shorter than two lengths of the vessel. The resulting process perturbations are treated as additional disturbances. The influence of waves was modeled in the form of a shaping filter driven by white noise [1].

In the ship simulation model, the steering gear was taken into account. However, during the controller synthesis process, its dynamics, as relatively small, was neglected.

## VII. CONCLUSION

Based on the Davidson and Schiff model of a ship augmented by linearized equations of its kinematics, a robust and adaptive ship steering system along a preset path is proposed. This disturbance-resistant system has been examined using a realistic, full, nonlinear simulation model of the training ship 'Blue Lady', taking into account various environmental disturbances. Good control performance has been achieved despite unknown dynamics of the controlled object.

## APPENDIX

We now present the main details and parameters of the ship that was used as a test object for the control algorithm presented in this study. The training ship '*Blue Lady*' is an isomorphic model of a real tanker made to 1:24 scale [12], [13].

We assume here that out of many actuators installed on the ship, we actually use the rudder and main propulsion only; therefore, we apply only the surge force and the yaw moment as available control signals. Such equipment is quite typical for many supply vessels [3].

In this part we will provide: (i) the proof of theorem of Section II, B. (cf. [16]), (ii) its extension that addresses the parameter drift problem; and (iii) the condition guaranteeing system stabilizability i.e. preventing $\hat{g}(\boldsymbol{x}, \hat{\boldsymbol{\theta}}^g)$ of zero-crossing.

(i) Let us define a Lyapunov function

$$V = \frac{1}{2}\boldsymbol{e}^T\boldsymbol{P}\boldsymbol{e} + \frac{1}{2\gamma_1}\tilde{\boldsymbol{\theta}}^{fT}\tilde{\boldsymbol{\theta}}^f + \frac{1}{2\gamma_2}\tilde{\boldsymbol{\theta}}^{gT}\tilde{\boldsymbol{\theta}}^g. \tag{1A}$$

The time derivative of $V$ is

$$\dot{V} = \frac{1}{2}\dot{\boldsymbol{e}}^T\boldsymbol{P}\boldsymbol{e} + \frac{1}{2}\boldsymbol{e}^T\boldsymbol{P}\dot{\boldsymbol{e}} + \frac{1}{\gamma_1}\tilde{\boldsymbol{\theta}}^{fT}\dot{\tilde{\boldsymbol{\theta}}}^f + \frac{1}{\gamma_2}\tilde{\boldsymbol{\theta}}^{gT}\dot{\tilde{\boldsymbol{\theta}}}^g. \tag{2A}$$

By the fact $\dot{\tilde{\boldsymbol{\theta}}}^f = -\dot{\hat{\boldsymbol{\theta}}}^f$, $\dot{\tilde{\boldsymbol{\theta}}}^g = -\dot{\hat{\boldsymbol{\theta}}}^g$ and (14) and (20), the above equation becomes

$$\begin{aligned}
\dot{V} &= \frac{1}{2}\Big[\boldsymbol{e}^T\boldsymbol{A}^T\boldsymbol{P}\boldsymbol{e} - \frac{1}{r}\boldsymbol{e}^T\boldsymbol{P}\boldsymbol{B}\boldsymbol{B}^T\boldsymbol{P}\boldsymbol{e} + \boldsymbol{w}^{fT}\tilde{\boldsymbol{\theta}}^f\boldsymbol{B}^T\boldsymbol{P}\boldsymbol{e} \\
&\quad + u\boldsymbol{w}^{gT}\tilde{\boldsymbol{\theta}}^g\boldsymbol{B}^T\boldsymbol{P}\boldsymbol{e} + \tilde{d}\boldsymbol{B}^T\boldsymbol{P}\boldsymbol{e} + \boldsymbol{e}^T\boldsymbol{P}\boldsymbol{A}\boldsymbol{e} - \frac{1}{r}\boldsymbol{e}^T\boldsymbol{P}\boldsymbol{B}\boldsymbol{B}^T\boldsymbol{P}\boldsymbol{e} \\
&\quad + \boldsymbol{e}^T\boldsymbol{P}\boldsymbol{B}\tilde{\boldsymbol{\theta}}^{fT}\boldsymbol{w}^f + \boldsymbol{e}^T\boldsymbol{P}\boldsymbol{B}\tilde{\boldsymbol{\theta}}^{gT}\boldsymbol{w}^g u + \boldsymbol{e}^T\boldsymbol{P}\boldsymbol{B}\tilde{d}\Big] \\
&\quad + \frac{1}{\gamma_1}\tilde{\boldsymbol{\theta}}^{fT}\dot{\tilde{\boldsymbol{\theta}}}^f + \frac{1}{\gamma_2}\tilde{\boldsymbol{\theta}}^{gT}\dot{\tilde{\boldsymbol{\theta}}}^g \\
&= \frac{1}{2}\boldsymbol{e}^T\left[\boldsymbol{P}\boldsymbol{A} + \boldsymbol{A}^T\boldsymbol{P} - \frac{2}{r}\boldsymbol{P}\boldsymbol{B}\boldsymbol{B}^T\boldsymbol{P}\right]\boldsymbol{e} \\
&\quad + \left(\boldsymbol{e}^T\boldsymbol{P}\boldsymbol{B}\boldsymbol{w}^{fT} + \frac{1}{\gamma_1}\dot{\tilde{\boldsymbol{\theta}}}^{fT}\right)\tilde{\boldsymbol{\theta}}^f + \left(\boldsymbol{e}^T\boldsymbol{P}\boldsymbol{B}\boldsymbol{w}^{gT}u + \frac{1}{\gamma_2}\dot{\tilde{\boldsymbol{\theta}}}^{gT}\right)\tilde{\boldsymbol{\theta}}^g \\
&\quad + \frac{1}{2}\left(\tilde{d}\boldsymbol{B}^T\boldsymbol{P}\boldsymbol{e} + \boldsymbol{e}^T\boldsymbol{P}\boldsymbol{B}\tilde{d}\right).
\end{aligned} \tag{3A}$$

Considering that $ru_\alpha^2 = r^{-1}\boldsymbol{e}^T\boldsymbol{P}\boldsymbol{B}\boldsymbol{B}^T\boldsymbol{P}\boldsymbol{e}$, from adaptive laws (21) and the Riccati-like equation (22), we get

$$\begin{aligned}
\dot{V} &= -\frac{1}{2}(\boldsymbol{e}^T\boldsymbol{Q}\boldsymbol{e} + ru_\alpha^2) - \frac{1}{2\rho^2}\boldsymbol{e}^T\boldsymbol{P}\boldsymbol{B}\boldsymbol{B}^T\boldsymbol{P}\boldsymbol{e} \\
&\quad + \frac{1}{2}\left(\tilde{d}\boldsymbol{B}^T\boldsymbol{P}\boldsymbol{e} + \boldsymbol{e}^T\boldsymbol{P}\boldsymbol{B}\tilde{d}\right) \\
&= -\frac{1}{2}(\boldsymbol{e}^T\boldsymbol{Q}\boldsymbol{e} + ru_\alpha^2) - \frac{1}{2}\left(\frac{1}{\rho}\boldsymbol{B}^T\boldsymbol{P}\boldsymbol{e} - \rho\tilde{d}\right)^T\left(\frac{1}{\rho}\boldsymbol{B}^T\boldsymbol{P}\boldsymbol{e} - \rho\tilde{d}\right) \\
&\quad + \frac{1}{2}\rho^2\tilde{d}^2 \le -\frac{1}{2}(\boldsymbol{e}^T\boldsymbol{Q}\boldsymbol{e} + ru_\alpha^2) + \frac{1}{2}\rho^2\tilde{d}^2
\end{aligned} \tag{4A}$$

Integrating the above equation from $t = 0$ to $t = T$ yields

$$V(T) - V(0) \le -\frac{1}{2}\int_0^T (\boldsymbol{e}^T\boldsymbol{Q}\boldsymbol{e} + ru_\alpha^2)dt + \frac{1}{2}\rho^2\int_0^T \tilde{d}^2 dt. \tag{5A}$$

Since $V(T) \ge 0$ the (5A) implies the following inequality

$$\frac{1}{2}\int_0^T (\boldsymbol{e}^T\boldsymbol{Q}\boldsymbol{e} + ru_\alpha^2)dt \le V(0) + \frac{1}{2}\rho^2\int_0^T \tilde{d}^2 dt. \tag{6A}$$

From (1A), the above inequality is equivalent to the following

$$\begin{aligned}\frac{1}{2}\int_0^T (\boldsymbol{e}^T\boldsymbol{Q}\boldsymbol{e} + ru_\alpha^2)dt \\ \leq \frac{1}{2}\boldsymbol{e}^T(0)\boldsymbol{P}\boldsymbol{e}(0) + \frac{1}{\gamma_1}\tilde{\boldsymbol{\theta}}^{fT}(0)\tilde{\boldsymbol{\theta}}^f(0) + \frac{1}{\gamma_2}\tilde{\boldsymbol{\theta}}^{gT}(0)\tilde{\boldsymbol{\theta}}^g(0) \\ + \frac{1}{2}\rho^2\int_0^T \tilde{d}^2 dt \end{aligned} \tag{7A}$$

Thus we have (17).

(ii) According to *Remark 1*. the theorem ensures perfect tracking i.e. $\lim_{t\to\infty} \boldsymbol{e}(t) = 0$ under assumption that $\int_0^\infty \tilde{d}^2 dt \leq M$. However, to cope with the parametric drift problem, leading to a blow-up phenomenon [22], we prove a variant of this theorem that guarantees ultimately uniform boundedness (UBB) [23], [24] of the closed-loop system under assumption that the total disturbance bound is $\left|\tilde{d}\right| \leq \beta$, where the constant $\beta > 0$ is not available.

To this end, we introduce into the adaptation laws (21) so-called $\sigma$-modification term obtaining

$$\begin{aligned}\dot{\hat{\boldsymbol{\theta}}}^f &= \gamma_1(\boldsymbol{w}^f\boldsymbol{B}^T\boldsymbol{P}\boldsymbol{e} - \sigma\hat{\boldsymbol{\theta}}^f) \\ \dot{\hat{\boldsymbol{\theta}}}^g &= \gamma_2(\boldsymbol{w}^g\boldsymbol{B}^T\boldsymbol{P}\boldsymbol{e}u - \sigma\hat{\boldsymbol{\theta}}^g)\end{aligned} \tag{8A}$$

Considering again the fact that $\dot{\tilde{\boldsymbol{\theta}}}^f = -\dot{\hat{\boldsymbol{\theta}}}^f$, $\dot{\tilde{\boldsymbol{\theta}}}^g = -\dot{\hat{\boldsymbol{\theta}}}^g$ and substituting (8A) to (3A) the formula (4A) will take a form

$$\begin{aligned}\dot{V} &= -\frac{1}{2}(\boldsymbol{e}^T\boldsymbol{Q}\boldsymbol{e} + ru_\alpha^2) - \frac{1}{2\rho^2}\boldsymbol{e}^T\boldsymbol{P}\boldsymbol{B}\boldsymbol{B}^T\boldsymbol{P}\boldsymbol{e} \\ &\quad + \frac{1}{2}\left(\tilde{d}\boldsymbol{B}^T\boldsymbol{P}\boldsymbol{e} + \boldsymbol{e}^T\boldsymbol{P}\boldsymbol{B}\tilde{d}\right) + \sigma(\tilde{\boldsymbol{\theta}}^{fT}\hat{\boldsymbol{\theta}}^f + \tilde{\boldsymbol{\theta}}^{gT}\hat{\boldsymbol{\theta}}^g) \\ &= -\frac{1}{2}(\boldsymbol{e}^T\boldsymbol{Q}\boldsymbol{e} + ru_\alpha^2) - \frac{1}{2}\left(\frac{1}{\rho}\boldsymbol{B}^T\boldsymbol{P}\boldsymbol{e} - \rho\tilde{d}\right)^T\left(\frac{1}{\rho}\boldsymbol{B}^T\boldsymbol{P}\boldsymbol{e} - \rho\tilde{d}\right) \\ &\quad + \frac{1}{2}\rho^2\tilde{d}^2 + \sigma(\tilde{\boldsymbol{\theta}}^{fT}(\boldsymbol{\theta}^{f*} - \tilde{\boldsymbol{\theta}}^f) + \tilde{\boldsymbol{\theta}}^{gT}(\boldsymbol{\theta}^{g*} - \tilde{\boldsymbol{\theta}}^g)) \\ &\leq -\frac{1}{2}(\lambda_{\min}(\boldsymbol{Q})\left\|\boldsymbol{e}\right\|^2 + ru_\alpha^2) + \frac{1}{2}\rho^2\tilde{d}^2 \\ &\quad + \sigma(\tilde{\boldsymbol{\theta}}^{fT}\boldsymbol{\theta}^{f*} - \left\|\tilde{\boldsymbol{\theta}}^f\right\|^2) + \sigma(\tilde{\boldsymbol{\theta}}^{gT}\boldsymbol{\theta}^{g*} - \left\|\tilde{\boldsymbol{\theta}}^g\right\|^2)\end{aligned} \tag{9A}$$

Based on identity

$$-x^2 + xy = -\frac{1}{2}(x-y)^2 - \frac{x^2}{2} + \frac{y^2}{2} \tag{10A}$$

we obtain

$$\begin{aligned}\tilde{\boldsymbol{\theta}}^T\boldsymbol{\theta}^* - \left\|\tilde{\boldsymbol{\theta}}\right\|^2 &\leq \left\|\tilde{\boldsymbol{\theta}}\right\|\left\|\boldsymbol{\theta}^*\right\| - \left\|\tilde{\boldsymbol{\theta}}\right\|^2 \\ &= -\frac{1}{2}\left(\left\|\tilde{\boldsymbol{\theta}}\right\| - \left\|\boldsymbol{\theta}^*\right\|\right)^2 - \frac{1}{2}\left(\left\|\tilde{\boldsymbol{\theta}}\right\|^2 - \left\|\boldsymbol{\theta}^*\right\|^2\right) \\ &\leq -\frac{1}{2}\left(\left\|\tilde{\boldsymbol{\theta}}\right\|^2 - \left\|\boldsymbol{\theta}^*\right\|^2\right)\end{aligned} \tag{11A}$$

Using (11A), the formula (9A) will take the form

$$\begin{aligned}\dot{V} &\leq -\frac{1}{2}(\lambda_{\min}(\boldsymbol{Q})\left\|\boldsymbol{e}\right\|^2 + ru_\alpha^2) \\ &\quad - \frac{1}{2}\sigma\left(\left\|\tilde{\boldsymbol{\theta}}^f\right\|^2 - \left\|\boldsymbol{\theta}^{f*}\right\|^2\right) \\ &\quad - \frac{1}{2}\sigma\left(\left\|\tilde{\boldsymbol{\theta}}^g\right\|^2 - \left\|\boldsymbol{\theta}^{g*}\right\|^2\right) + \frac{1}{2}\rho^2\tilde{d}^2 \\ &= \underbrace{-\frac{1}{2}(\lambda_{\min}(\boldsymbol{Q})\left\|\boldsymbol{e}\right\|^2 + ru_\alpha^2) - \frac{1}{2}\sigma\left(\left\|\tilde{\boldsymbol{\theta}}^f\right\|^2 + \left\|\tilde{\boldsymbol{\theta}}^g\right\|^2\right)}_{(a)} \\ &\quad + \frac{1}{2}\sigma\left(\left\|\boldsymbol{\theta}^{f*}\right\|^2 + \left\|\boldsymbol{\theta}^{g*}\right\|^2\right) + \frac{1}{2}\rho^2\tilde{d}^2\end{aligned} \tag{12A}$$

Considering that

$$\begin{aligned}V &= \frac{1}{2}\boldsymbol{e}^T\boldsymbol{P}\boldsymbol{e} + \frac{1}{2\gamma_1}\tilde{\boldsymbol{\theta}}^{fT}\tilde{\boldsymbol{\theta}}^f + \frac{1}{2\gamma_2}\tilde{\boldsymbol{\theta}}^{gT}\tilde{\boldsymbol{\theta}}^g \\ &\leq \frac{1}{2}\lambda_{\max}(\boldsymbol{P})\left\|\boldsymbol{e}\right\|^2 + \frac{1}{2\gamma_1}\left\|\tilde{\boldsymbol{\theta}}^f\right\|^2 + \frac{1}{2\gamma_2}\left\|\tilde{\boldsymbol{\theta}}^g\right\|^2\end{aligned} \tag{13A}$$

we relate (a) to $V$, thus (12A) can be further derived as

$$\begin{aligned}\dot{V} &\leq -\alpha V + \frac{1}{2}(\alpha\lambda_{\max}(\boldsymbol{P}) - \lambda_{\min}(\boldsymbol{Q}))\left\|\boldsymbol{e}\right\|^2 \\ &\quad + \frac{1}{2}\left(\frac{\alpha}{\gamma_1} - \sigma\right)\left\|\tilde{\boldsymbol{\theta}}^f\right\|^2 + \frac{1}{2}\left(\frac{\alpha}{\gamma_2} - \sigma\right)\left\|\tilde{\boldsymbol{\theta}}^g\right\|^2 \\ &\quad + \frac{1}{2}\sigma\left(\left\|\boldsymbol{\theta}^{f*}\right\|^2 + \left\|\boldsymbol{\theta}^{g*}\right\|^2\right) + \frac{1}{2}\rho^2\tilde{d}^2.\end{aligned} \tag{14A}$$

By picking

$$\alpha \leq \min\left\{\frac{\lambda_{\min}(\boldsymbol{Q})}{\lambda_{\max}(\boldsymbol{P})}, \gamma_1\sigma, \gamma_2\sigma\right\} \tag{15A}$$

we have

$$\dot{V} \leq -\alpha V + \frac{1}{2}\sigma\left(\left\|\boldsymbol{\theta}^{f*}\right\|^2 + \left\|\boldsymbol{\theta}^{g*}\right\|^2\right) + \frac{1}{2}\rho^2\tilde{d}^2. \tag{16A}$$

Hence $\dot{V} \leq 0$ whenever

$$\begin{aligned}\left(\boldsymbol{e}, \tilde{\boldsymbol{\theta}}\right) \in E = \left\{\left(\boldsymbol{e}, \tilde{\boldsymbol{\theta}}\right) : \quad V \geq \frac{1}{2\alpha}\left(\sigma\left(\left\|\boldsymbol{\theta}^{f*}\right\|^2 + \left\|\boldsymbol{\theta}^{g*}\right\|^2\right)\right.\right. \\ \left.\left. + \rho^2\sup_\tau \tilde{d}^2(\tau)\right)\right\}\end{aligned} \tag{17A}$$

This implies that $(\boldsymbol{e}, \tilde{\boldsymbol{\theta}})$ is UUB. Note that the size of the set $E$ is adjustable by proper choice of $\alpha$, $\sigma$, $\boldsymbol{P}$, $\boldsymbol{Q}$. Smaller size $E$ results in more accurate output tracking. However, this parameter tuning is not always unlimited, as it may cause controller saturation during the implementation.

(iii) At this point we will present a modified tuning law (49) that would guarantee that $\hat{g}(\boldsymbol{x}, \hat{\boldsymbol{\theta}}^g)$ of (7) or estimates $\hat{\boldsymbol{\theta}}^g$ of (19) are bounded away from zero. This problem can be solved by 'projection modification' method [22], [23], [25].

$$\dot{\hat{\theta}}_1^g = \begin{cases}\gamma_4\varepsilon\delta, & if \quad \left|\hat{\theta}_1^g\right| > \theta_{\min}^g \vee \left[\hat{\theta}_1^g = \theta_{\min}^g sgn\theta_1^{g*} \wedge (\varepsilon\delta)sgn\theta_1^{g*} > 0\right] \\ 0, & if \quad \left|\hat{\theta}_1^g\right| = \theta_{\min}^g \wedge (\varepsilon\delta)sgn\theta_1^{g*} < 0\end{cases} \tag{18A}$$

Taking advantage of the fact that in our case $\hat{g}(\boldsymbol{x}, \hat{\boldsymbol{\theta}}^g)$ in (45) is a scalar function $\hat{\theta}_1^g(t)$, the general projection modification formula takes the following simple form (18A), as shown at the bottom of the previous page, where $\theta_1^{g*} = b_1 + kb_2$ (cf. (41)). We also assume that $sgn\theta_1^{g*}$ is known and $\theta_{\min}^g$ represents a known lower bound of $\left|\hat{\theta}_1^g\right|$. This formula can be combined with the $\sigma$-modification term [22].

The main goal here is to stop adaptation of $\hat{\theta}_1^g$ if the parameter reaches its lower absolute limit value $\hat{\theta}_{\min}^g$, with a nonzero time derivative $\dot{\hat{\theta}}_1^g$. The formal but elementary proof of (18A), can be found e.g. in [25].

## REFERENCES


[1] T. I. Fossen, *Guidance and Control of Ocean Vehicles*. Chichester, NH, USA: Wiley, 1994.

[2] J. Ghommam, S. E. Ferik, and M. Saad, "Robust adaptive path-following control of underactuated marine vessel with off-track error constraint," *Int. J. Syst. Sci.*, vol. 49, no. 7, pp. 1540–1558, May 2018.

[3] E. Lefeber, K. Y. Pettersen, and H. Nijmeijer, "Tracking control of an underactuated ship," *IEEE Trans. Control Syst. Technol.*, vol. 11, no. 1, pp. 52–60, Jan. 2003.

[4] T. Holzhüter, "LQG approach for the high-precision track control of ships," *IEE Proc.-Control Theory Appl.*, vol. 144, no. 2, pp. 121–127, Mar. 1997.

[5] R. Zhang, Y. Chen, Z. Sun, F. Sun, and H. Xu, "Path control of a surface ship in restricted waters using sliding mode," *IEEE Trans. Control Syst. Technol.*, vol. 8, no. 4, pp. 722–732, Jul. 2000.

[6] Z. Hui and S. Jihong, "Path following control of underactuated ship based on nonlinear backstepping," in *Proc. IEEE Int. Conf. Inf. Autom. (ICIA)*, Yinchuan, China, Aug. 2013, pp. 1–6.

[7] D. B. Dačić and P. V. Kokotović, "Path-following for linear systems with unstable zero dynamics," *Automatica*, vol. 42, no. 10, pp. 1673–1683, Oct. 2006.

[8] K. D. Do, Z. P. Jiang, and J. Pan, "Robust adaptive path following of underactuated ships," *Automatica*, vol. 40, no. 6, pp. 929–944, Jun. 2004.

[9] Z. Liu, "Practical backstepping control for underactuated ship path following associated with disturbances," *IET Intell. Transp. Syst.*, vol. 13, no. 5, pp. 834–840, May 2019.

[10] J. E. Slotine and W. Li, *Applied Nonlinear Control*. Englewood Cliffs, NJ, USA: Prentice-Hall, 1991, pp. 246–265.

[11] Z. Zwierzewicz, "Nonlinear adaptive tracking-control synthesis for functionally uncertain systems," *Int. J. Adapt. Control Signal Process.*, vol. 24, no. 2, pp. 96–105, Feb. 2010.

[12] M. Tomera, *Switching-Based Multi-Operational Control of Ship Motion*. New York, NY, USA: Academic, 2018.

[13] M. Tomera, "Controlling the physical model of the tanker along a preset path of passage," (Sterowanie modelem fizycznym zbiornikowca wzdłuż zadanej trasy przejścia), Zeszyty Naukowe Wydziału Elektrotechniki i Automatyki Politechniki Gdańskiej (in Polish), Gdańsk, Poland, Tech. Rep. 51/2016, 2016.

[14] Z. Zwierzewicz, "Robust and adaptive ship path-following control design with the full vessel model," in *Proc. 24th Int. Conf. Methods Models Autom. Robot. (MMAR)*, Międzyzdroje, Poland, Aug. 2019, pp. 121–126.

[15] A. P. Aguiar, J. P. Hespanha, and P. V. Kokotovic, "Path-following for non-minimum phase systems removes performance limitations," *IEEE Trans. Autom. Control*, vol. 50, no. 2, pp. 234–239, Feb. 2005.

[16] B.-S. Chen, C.-H. Lee, and Y.-C. Chang, "H$^\infty$ tracking design of uncertain nonlinear SISO systems: Adaptive fuzzy approach," *IEEE Trans. Fuzzy Syst.*, vol. 4, no. 1, pp. 32–43, 1st Quart., 1996.

[17] G. G. Rigatos, "Adaptive control methods for industrial systems," in *Modelling and Control for Intelligent Industrial Systems* (Intelligent Systems Reference Library), vol. 7. Berlin, Germany: Springer-Verlag, 2011, ch. 4, pp. 65–96.

[18] M. Abu-Khalaf, J. Huang, and F. L. Lewis, *Nonlinear H2/H-Infinity Constrained Feedback Control* (Advances in Industrial Control). London, U.K.: Springer, 2006.

[19] R. Skjetne, R. Smogeli, and T. I. Fossen, "Modeling, identification, and adaptive maneuvering of cybership II: A complete design with experiments," in *Proc. IFAC Conf. Control Appl. Mar. Syst.*, Ancona, Italy, Jul. 2004, pp. 203–208.

[20] H. K. Khalil, *Nonlinear Systems*. Upper Saddle River, NJ, USA: Prentice-Hall, 2002, pp. 509–521.

[21] *Control System Toolbox Documentation*. Accessed: Mar. 25, 2019. [Online]. Available: https://www.mathworks.com/help/control

[22] J. A. Farrell and M. M. Polycarpou, *Adaptive Approximation Based Control: Unifying Neural, Fuzzy and Traditional Adaptive Approximation Approaches*. Hoboken, NJ, USA: Wiley, 2006.

[23] C. L. Hwang, C. C. Chiang, and Y. W. Yeh, "Adaptive fuzzy hierarchical sliding-mode control for the trajectory tracking of uncertain under-actuated nonlinear dynamic systems," *IEEE Trans. Fuzzy Syst.*, vol. 22, no. 2, pp. 286–297, Apr. 2014.

[24] C.-L. Hwang, Y.-M. Chen, and C. Jan, "Trajectory tracking of large-displacement piezoelectric actuators using a nonlinear observer-based variable structure control," *IEEE Trans. Control Syst. Technol.*, vol. 13, no. 1, pp. 56–66, Jan. 2005.

[25] E. Lavretsky and K. Wise, *Robust and Adaptive Control: With Aerospace Applications*. Springer 2013.



**ZENON ZWIERZEWICZ** received the M.Sc. degree in mathematics from Szczecin University, Szczecin, Poland, in 1978, the Ph.D. degree in automatic control from the Technical University of Szczecin, in 1986, and the D.Sc. degree in automatic control from the University of Rostock, Germany, in 1994.

He is currently a Professor with the Faculty of Mechatronics and Electrical Engineering, Maritime University of Szczecin. His research interests include control and systems theory, including nonlinear and optimal control, adaptive and intelligent control, and autonomous systems control.